Stochastic Optimization Formulations for Wind Turbine Power Maximization and Extreme Load Mitigation

Yankai Cao, Fernando D'Amato, and Victor M. Zavala

***Abstract*—We propose stochastic optimization formulations to identify optimal parameters for pitch and torque controllers in wind turbines. The approach seeks to extract maximum power and to satisfy extreme mechanical load requirements by design. The proposed formulation incorporates a wind turbine dynamic model, control law representations for pitch and torque controllers, and a probabilistic constraint that captures the long-term probability of exceeding an extreme load threshold (as described by the IEC-61400). We use the fact that the extreme load follows a generalized extreme value distribution to obtain an explicit algebraic characterization of the probabilistic constraint. The proposed approach can find controller parameters that increase power output relative to a nominal control design without changing the structure of existing controllers and while maintaining the original extreme load characteristics. We also demonstrate that the optimization formulation, which is cast as a large-scale nonlinear programming problem with up to 7.5 million variables and constraints, can be solved in less than 1.5 hours using a state-of-the-art parallel interior-point solver.**

***Index Terms*—Stochastic, optimization, extreme load mitigation, wind turbines.**

I. Introduction

INDUSTRIAL wind turbines are designed to operate through a lifetime of more than 15 years subject to uncertain weather. Strong wind conditions that are expected to happen during this lifetime could compromise the turbine's integrity, if not properly handled through the control system. To prevent structural damage and high life consumption rates, the International Electrotechnical Commission (IEC) standards require wind turbine designers to ensure that the turbine does not exceed critical load conditions when subject to a multiplicity of hypothetical operating scenarios. Many of these critical load conditions are derived using statistical load extrapolation methods [1], [2], [3] that seek to use limited wind data to assess the long-term probability of the turbine of exceeding a certain load threshold. Load extrapolation techniques are based on a powerful result from extreme value theory that states that the maximum of a sequence of independent random variables (i.e., the loads) follows a generalized extreme value distribution. The existence of the extreme value distribution allows practitioners to estimate the probability of rare long-term events. This is an analog of the celebrated central limit theorem that states that the sum of independent random variables follows a normal distribution.

Yankai Cao and Victor M. Zavala are with the Department of Chemical and Biological Engineering,University of Wisconsin-Madison, 1415 Engineering Dr, Madison, WI 53706, USA (e-mail: victor.zavala@wisc.edu).

Fernando D'Amato is with General Electric Global Research,1 Research Cir, Niskayuna, NY 12309, USA (e-mail: damato@ge.com).

Controlling the operation of an industrial wind turbine requires a careful tradeoff between energy capture and compliance with structural loads. Control strategies for industrial wind turbines are typically based on control laws that regulate power and rotor speed by operating generator torque and collective blade pitch angle. In addition, multiple control laws are added to mitigate loads [4], [5]. As a result, designing a viable controller involves iterative tuning multiple control parameters until it satisfies the requirements of the IEC standard. This process is tedious and computationally expensive.

Recent research activity [6], [7], [8], [9], [10] has been focusing on Model Predictive Control (MPC) technology to handle regulation controls for power and speed as well as time domain constraints typical from the IEC standard. MPC is a powerful optimization-based control technology that can aid standard controllers, as it can directly accommodate detailed turbine models and constraints of different forms and with this anticipate wind events and capture multivariable interactions. In particular, MPC strategies can perform simultaneous blade pitch and generator torque control while maximizing power and mitigating extreme loads. For instance, in the work of [6], it is shown that under an extreme gust event, an MPC strategy can reduce the tower base moment by up to 15% compared to standard controllers. Similarly, the work of [7] uses a nonlinear MPC formulation to demonstrate that some loads can be reduced by up to 50% under extreme gusts without negative impact on overall power production. The nonlinear MPC formulation of [10] also shows that it can reduce the tower bending moment by up to 40%. Simplified MPC strategies have also been reported in the literature that seek to overcome computational complexity by using linearized model representations [8], [9]. A limitation of MPC strategies reported in the literature is that they analyze robustness to diverse wind events on a case by case basis and do not capture long-term extreme load constraints as required by IEC standards. Unfortunately, the computational procedures needed to fit operational loads to extreme value distributions and to predict long-term extreme loads are complex and not trivial to implement in MPC formulations. Because of this, the effect of control strategies on wind turbine loads is often performed *a posteriori* and not *a priori* by design.

The main contribution of this work is the proposal of a stochastic optimization framework to obtain pitch and torque controller parameters that maximize power while enforcing extreme load constraints as required by IEC standards. The formulation incorporates a simplified nonlinear wind turbine model and extracts load maxima from multiple wind field scenarios to estimate a long-term probability of load threshold violation. In addition, the formulation is used to evaluate a

best hypothetical supervisory strategy, that can be used as a reference metric for the maximum achievable performance. The methodology is benchmarked against simplified control strategies proposed in the literature [10], [11] that define parameters for the pitch and torque control laws operating mostly at rated conditions. We also show that the stochastic optimization formulation, which is cast as a large-scale nonlinear program with up to 7.5 million variables, can be solved in less than 1.3 hours by using a state-of-the-art parallel optimization solver. We also provide evidence that the approach can find controller parameters that increase power output relative to a nominal control design without changing the structure of existing controllers and while maintaining the original extreme load characteristics.

II. Optimization Formulations

In this section, we present a deterministic and a stochastic formulation for the wind turbine power maximization problem. The goal in the deterministic formulation is to calculate optimal controller parameters that maximize the wind turbine power. We also impose constraints on the maximum load experienced by the turbine under a given known wind speed profile. In the stochastic optimization formulation, the goal is to calculate optimal controller parameters that maximize expected power over an uncertain wind power profile (where uncertainty is captured in the form of scenarios). The stochastic formulation also imposes probabilistic constraints for the exceedance of given load thresholds in the long-term loads. The probabilistic constraint uses the methodology required by the IEC61400-1 standard. The formulations also capture physical dynamics of the turbine and incorporate controller laws. Appendix A describes all variables, parameters, and units of the model.

A. Wind Turbine Model

The dynamics of the wind turbine are described by the following system [10] of differential and algebraic equations (DAEs):

$$\dot{w_r}(t) = \frac{1}{J}(M_z(t) - N_g T_{gen}(t)) \tag{II.1a}$$
$$\dot{x}(t) = v_x(t) \tag{II.1b}$$
$$\dot{v_x}(t) = \frac{1}{m_{Te}}(-c_{Te}v_x(t) - k_{Te}x(t) + F_z(t)) \tag{II.1c}$$
$$V_{rel}(t) = V(t) - v_x(t) \tag{II.1d}$$
$$\lambda(t) = w_r(t)R_r/V_{rel}(t) \tag{II.1e}$$
$$C_t(t) = \text{Thrust}(\theta(t), \lambda(t)) \tag{II.1f}$$
$$C_m(t) = \text{Torque}(\theta(t), \lambda(t)) \tag{II.1g}$$
$$F_z(t) = \frac{1}{2}\rho V_{rel}(t)^2 A C_t(t) \tag{II.1h}$$
$$M_z(t) = \frac{1}{2}\rho V_{rel}(t)^2 A R_r C_m(t)/\lambda(t) \tag{II.1i}$$
$$y_P(t) = T_{gen}(t)w_g(t)(1 - P_1) \tag{II.1j}$$
$$y_L(t) = H(k_{Te}x(t) + c_{Te}v_x(t)) \tag{II.1k}$$

Equations (II.1f) and (II.1g) are given by:

$$\begin{aligned} C_t(t) &= \text{Thrust}(\theta(t), \lambda(t)) \\ &= -0.001975\lambda(t)^2 - 7.64510^{-6}\theta(t)^2 \\ &\quad - 0.008423\theta(t)\lambda(t) + 0.009459\theta(t) \\ &\quad + 0.09179\lambda(t) + 0.1831 \end{aligned} \tag{II.2a}$$

$$\begin{aligned} C_m(t) &= \text{Torque}(\theta(t), \lambda(t)) \\ &= -0.005738\lambda(t)^2 - 7.57610^{-5}\theta(t)^2 \\ &\quad - 0.005538\theta(t)\lambda(t) + 0.005477\theta(t) \\ &\quad + 0.0944\lambda(t) + 0.1218 \end{aligned} \tag{II.2b}$$

These are nonlinear equations that were obtained by fitting look-up tables available in the literature [10].

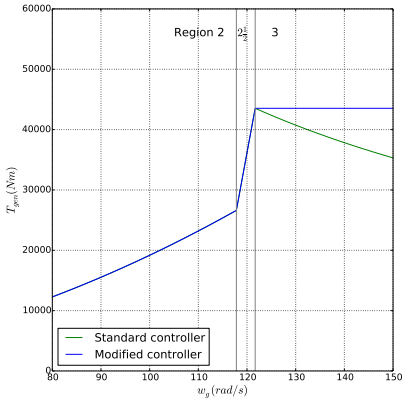

Fig. 1: **Standard and modified torque control laws.**

The wind turbine is equipped with *single-loop* controllers for torque $T_{gen}(t)$ and pitch angle $\theta(t)$. The *generator torque controller* used has the form proposed in [11]. Given a set-point for rated power P_{rated} and the generator speed $w_g(t) = w_r(t)N_g$, the controller adjusts the torque according to:

$$T_{gen}(t) = \begin{cases} \kappa w_g(t)^2, & \text{if } w_g(t) \le w_{g_2} \\ \kappa w_{g_2}^2 + \frac{w_g(t) - w_{g_2}}{w_{g_{25}} - w_{g_2}}\left(P_{rated}/w_{g_{25}} - \kappa w_{g_2}^2\right), & \\ \qquad \text{if } w_{g_2} < w_g(t) \le w_{g_{25}} & \\ P_{rated}/w_g(t), & \text{if } w_g(t) > w_{g_{25}} \end{cases} \tag{II.3}$$

where $\kappa > 0$ is a parameter. As shown in Fig. 1, the control law is piecewise linear (non-smooth) and has three regions of interest. The parameter w_{g_2} denotes the threshold between region 2 and region 2.5 and $w_{g_{25}}$ denotes the threshold between region 2.5 and region 3. This strategy defines the torque setpoints in region 3 to provide rated power.

For the *blade pitch controller*, we use a proportional-integral control law [11] that adjusts the pitch angle given a set-point for the generator speed ($w_{g_{ref}}$):

$$\Delta w_g(t) = w_g(t) - w_{g_{ref}} \tag{II.4a}$$
$$w_{g_{int}}(t) = \int_0^t \Delta w_g(\tau) d\tau \tag{II.4b}$$
$$w_{g_{int}}(t) = \max(w_{g_{int}}(t-1) + \Delta w_g(t)h, 0) \tag{II.4c}$$
$$\theta(t) = \max(K_P \Delta w_g(t) + K_I w_{g_{int}}(t), 0) \tag{II.4d}$$

and we use the parameters K_P = 0.216, K_I = 0.0924.

By using the control laws described before, the optimization problem has four degrees of freedom, given by the *controller parameters* $u = (P_{rated},\ w_{g_{ref}},\ w_{g_2}, w_{g_{25}})$. The parameters P_{rated}, w_{g_2}, and $w_{g_{25}}$ determine the performance of the local controller for torque, and $w_{g_{ref}}$ determines the performance of the pitch controller.

An alternative strategy for region 3 is given by the following modified torque control law, which allows power to go above rated values during short time intervals.

$$T_{gen}(t) = \begin{cases} \kappa w_g(t)^2, & \text{if } w_g(t) \le w_{g_2} \\ \kappa w_{g_b}^2 + \frac{w_g(t)-w_{g_b}}{w_{g_{25}}-w_{g_b}} \left(P_{rated}/w_{g_{25}} - \kappa w_{g_b}^2\right), & \\ \qquad \text{if} w_{g_2} < w_g(t) \le w_{g_{25}} & \\ P_{rated}/w_{g_{25}}, & \text{if } w_g(t) > w_{g_{25}}. \end{cases} \tag{II.5}$$

Here, instead of maintaining constant power in region 3, we adopt the strategy proposed in [10] to maintain the rated torque value whenever the rotor speed exceeds its rated value. We emphasize that the only difference between the modified and the standard control law is in region 3, as shown in Figure 1. In particular, in region 3 of the modified formulation, the generator torque remains constant as $w_g(t)$ increases, and thus the power output increases as $w_g(t)$ increases. In Section IV we show that this modification can increase performance.

B. Deterministic Optimization Formulation

We represent the deterministic wind turbine optimization problem in the following abstract form:

$$\max_{u\in\mathcal{U}} \frac{1}{T}\int_{\mathcal{T}} y_P(t)dt \tag{II.6a}$$

$$\text{s.t. } (y_P(t), y_L(t)) = \phi(u, V(t)),\ t \in \mathcal{T} \tag{II.6b}$$

$$y_L(t) \le \bar{y}_L,\ t \in \mathcal{T} \tag{II.6c}$$

where $t \in \mathcal{T} := [0, T]$, $y_P(t)$ is the wind turbine power, $y_L(t)$ is the mechanical load with associated threshold $\bar{y}_L$, and $V(t)$ is the wind profile. The controls u (the controller parameters) are restricted to the closed set $\mathcal{U}$, which is a four-dimensional hypercube defined by the following constraints:

$$P_{rated0} \le P_{rated} \le 1.2P_{rated0} \tag{II.7a}$$

$$w_{g_{ref0}} \le w_{g_{ref}} \le 1.2w_{g_{ref0}} \tag{II.7b}$$

$$w_{g250} \le w_{g_{25}} \le 1.2w_{g_{250}} \tag{II.7c}$$

$$w_{g_{20}} \le w_{g_2} \le 1.2w_{g_{20}}. \tag{II.7d}$$

An important practical problem is that power maximization often conflicts with the mechanical load experienced by the turbine (i.e., the higher the power extracted the higher the load). Consequently, it is critical to carefully trade-off these metrics so as to prevent putting the turbine at mechanical risk.

We also highlight that the optimization formulation is a *controller design* formulation that seeks to identify optimal parameters for the low-level torque and pitch controllers and allow the low-level controllers to act the pitch angle and torque to react to high-frequency wind variations. Additionally, we consider the problem of allowing MPC to directly compute the control actions on pitch and torque actuation, without the low level control loops. This approach although not suitable for practical implementation, can provide valuable information about achievable performance. We discuss this more advanced setting in Section IV.

C. Standard Stochastic Optimization Formulation

The deterministic formulation treats the wind profile as a known input and seeks to identify the controller parameters that maximize total power over the time horizon $[0, T]$ while keeping the load within the maximum threshold. To account for wind variability (see Figure 5), we use a stochastic formulation. We model the wind profile as a random variable $V(t)$ and use $V(t, \omega)$ to denote a realization $\omega \in \Omega$ obtained from the probability density $p(V(t))$. Here, Ω represents a scenario (or realization) set. We note that, because the wind profile propagates through the wind turbine model, the turbine extracted power and load outputs are also random variables. To maintain notational consistency, the random power output is denoted simply as $y_P(t)$ with realizations $y_P(t, \omega)$ and the random load is $y_L(t)$ with realizations $y_L(t, \omega)$. The *posterior probability density* of the power output and for the load are denoted as $p_P(y_P(t) \,|\, V(t), u)$ and $p_L(y_L(t) \,|\, V(t), u)$. Realizations from these posterior densities (denoted as $y_P(t, \omega)$ and $y_L(t, \omega)$) are obtained by propagating the wind speed realizations $V(t, \omega)$ and u through the model. We note that the posterior densities *do not have a closed form* due to the nonlinearity of the wind turbine model.

A standard stochastic formulation takes the form:

$$\max_{u\in\mathcal{U}} \mathbb{E}\left[\frac{1}{T}\int_{\mathcal{T}} y_P(t, \omega)dt\right] \tag{II.8a}$$

$$\text{s.t. } (y_P(t, \omega), y_L(t, \omega)) = \phi(u, V(t, \omega)),\ t \in \mathcal{T},\ \omega \in \Omega \tag{II.8b}$$

$$y_L(t, \omega) \le \bar{y}_L,\ t \in \mathcal{T}\ \omega \in \Omega. \tag{II.8c}$$

In this formulation, the load constraint is required to be satisfied in each possible scenario of the wind profile (the constraints are assumed to be enforced almost surely).

In a *probabilistic-constrained* stochastic formulation, we relax the load constraint by enforcing it only with a sufficiently small probability. This formulation takes the form:

$$\max_{u\in\mathcal{U}} \mathbb{E}\left[\frac{1}{T}\int_{\mathcal{T}} y_P(t, \omega)dt\right] \tag{II.9a}$$

$$\text{s.t. } (y_P(t, \omega), y_L(t, \omega)) = \phi(u, V(t)),\ t \in \mathcal{T},\ \omega \in \Omega \tag{II.9b}$$

$$\mathbb{P}\left\{y_L(t, \omega) \le \bar{y}_L,\ t \in \mathcal{T}\right\} \ge \alpha. \tag{II.9c}$$

where α is a probability level close to one. We note that the probabilistic constraint (II.9c) can also be expressed as $\mathbb{P}\left\{\max_{t\in\mathcal{T}} y_L(t, \omega) \le \bar{y}_L\right\} \ge \alpha$. This constraint enforces that the probability that the maximum load over the time horizon $\mathcal{T}$ exceeds the threshold is no more than $1 - \alpha$. Moreover, the cumulative density function of the extreme load $\max_{t\in\mathcal{T}} y_L(t, \omega)$ is denoted as $F_{max}(\hat{y}_L(\alpha)) = \mathbb{P}\left\{\max_{t\in\mathcal{T}} y_L(t, \omega) \le \hat{y}_L(\alpha)\right\}$, where $\hat{y}_L(\alpha)$ is the α-critical value (fractile/quartile) of the distribution. We refer to this critical load value as the *characteristic load*. The probabilistic constraint can also written as $F_{max}(\hat{y}_L(\alpha)) \ge \alpha$

or one can use the constraint on the quartile $\hat{y}_L(\alpha) \leq \bar{y}_L$. In particular, we note that $\hat{y}_L(\alpha) \leq \bar{y}_L$ implies $\mathbb{P}\{\max_{t\in\mathcal{T}} y_L(t,\omega) \leq \hat{y}_L(\alpha)\} \geq \alpha$.

The stochastic formulation (II.9) enforces the probabilistic load constraint over the time domain $\mathcal{T}$. Clearly, if rare and extreme load scenarios over horizons of years need to be captured, this approach would be computationally impractical. Moreover, the conditional density $F_{max}(\cdot)$ does not have a closed form due to the nonlinearity of the wind turbine model. We now describe a procedure to approximate this long-term probabilistic constraint by using load extrapolation methods.

D. Stochastic Formulation Based on Statistical Extrapolation

The IEC-61400 standard proposes a procedure to enforce long-term (1-year and 50-year) probabilistic constraints on extreme loads. This is done by using existing short-term load data to perform long-term extrapolation [1] and gives a special type of *probabilistic load constraint* that can be implemented computationally. This method has been shown to provide accurate estimates of long-term extreme loads [2], [3].

In this section we provide a summary of load extrapolation procedures. The key idea behind load extrapolation is to define a sufficiently long horizon (that we also define as $\mathcal{T}$ with some abuse of notation) under which the extreme load $\max_{t\in\mathcal{T}} y_L(t,\omega)$ achieves statistical steady-state and with this ensure that it becomes statistically independent of the extreme load at a subsequent time horizon $\mathcal{T}'$. With this, we can split a long horizon of interest into a set of short time horizons and define the extreme load over the long horizon as the maximum of the extreme loads over the short horizons (because the maximum loads over the short horizons are statistically independent). The length of the short horizon is typically chosen to be 10 minutes [1]. Load extrapolation methods are based on the crucial observation that the maximum of a set of independent random variables distributes according to the generalized extreme value distribution (here we focus on the Gumbel distribution, which is a special case).

The *peak-over-threshold* procedure to estimate the characteristic extreme loads is summarized as follows:

- Each realization of the wind $V(t,\omega), t \in \mathcal{T}$ has an associated time-average wind speed $\bar{V}$. We discretize the time-average wind-speed range into $j \in \mathcal{B} := \{1, ..., B\}$ bins (the bins typically span the range $[3, 25]$ m/s and we use B =23 bins). We categorize every realization of the wind into a single bin j with corresponding mean wind speed $\bar{V}_j$ and create scenario sets Ω_j with $\Omega = \cup_{j\in\mathcal{B}}\Omega_j$.
- For a given wind speed bin $\bar{V}_j$, we gather wind turbine power realizations under fixed controller parameters u and N_j wind profiles from the scenario set Ω_j. These realizations have associated loads $y_L(t,\omega)$, $\omega \in \Omega_j$ from which we extract a total of n_j local load maxima that are contained in a vector $L_j \in \Re^{n_j}$. The maxima are defined as all local load maxima above a given threshold $\hat{L}_j$.
- Fit the local maxima to a Gumbel distribution. The parameters of the Gumbel distribution are:

$$c_j = \frac{\sqrt{6}\,\sigma_j}{\pi},\ j \in \mathcal{B} \tag{II.10a}$$

$$L_j^0 = \overline{L}_j - c_j\gamma,\ j \in \mathcal{B}. \tag{II.10b}$$

  where σ_j is the standard deviation of L_j, $\overline{L}_j$ is the mean of L_j, and γ is the Euler constant.
- We compute the long-term exceedance probability for the load $P_{ex}(y_L)$ by integrating over all operating wind speeds. This is done using the equations:

$$F_j(y_L) = \exp - \left(\exp - \left(\frac{y_L - L_j^0}{c_j}\right)\right),\ j \in \mathcal{B} \tag{II.11a}$$

$$P_{ex}(y_L) = \sum_{j\in\mathcal{B}} p_j(1 - F_j(y_L)^{n_j}). \tag{II.11b}$$

  Here, $F_j(\cdot)$ is cumulative Gumbel density function (probability that the load is below the critical value y_L) conditional to the mean speed $\bar{V}_j$ and p_j is the probability that the mean wind speed is within the bin $j \in \mathcal{B}$. The probabilities can be computed if we assume that the mean wind speed follows a Rayleigh distribution.
- We solve the equation $P_{ex}(y_L) = \alpha_{50yr}$ with $\alpha_{50yr} = \frac{10}{50\times365\times24\times60} = 3.8\times10^{-7}$ for y_L to obtain the 50-year *characteristic load* $\hat{y}_L(\alpha_{50yr})$ or solve $P_{ex}(y_L) = \alpha_{1yr}$ with $\alpha_{1yr} = \frac{10}{1\times365\times24\times60} = 1.9\times10^{-5}$ for y_L to obtain the 1-year load $\hat{y}_L(\alpha_{1yr})$.

We highlight that the characteristic load $\hat{y}_L(\alpha)$ is the critical load (a fractile) that exceeds the threshold $\bar{y}_L$ with probability α. The 50-year characteristic load is to be interpreted as the load that, on average, is *exceeded only once every 50 years*. Similarly, the 1-year load is to be interpreted as the load that, on average, is exceeded only once every one year.

In a simulation setting, we obtain wind turbine realizations of the loads $y_L(t,\omega)$ by performing model simulations. The IEC-61400 load extrapolation procedure can thus be represented by using an input-output function of the form:

$$\hat{y}_L(\alpha) = \varphi(y_L(\cdot,\cdot)) \tag{II.12}$$

where $\hat{y}_L(\alpha)$ is the characteristic load at probability level α (e.g., 1-year, 20-year, 50-year). With this, we can define an abstract stochastic optimization problem of the form:

$$\max_{u\in\mathcal{U}} \mathbb{E}\left[\frac{1}{T}\int_{\mathcal{T}} y_P(t,\omega)dt\right] \tag{II.13a}$$

$$\text{s.t. } (y_P(t,\omega), y_L(t,\omega)) = \phi(u, V(t,\omega)),\ t \in \mathcal{T},\ \omega \in \Omega \tag{II.13b}$$

$$\hat{y}_L(\alpha) = \varphi(y_L(\cdot,\cdot)) \tag{II.13c}$$

$$\hat{y}_L(\alpha) \leq \bar{y}_L. \tag{II.13d}$$

Here, constraint (II.13d) requires that the characteristic load obtained with the extrapolation procedure satisfies the maximum load threshold $\bar{y}_L$. This constraint on the fractile $\hat{y}_L(\alpha)$ implies that the probability that the load exceeding the threshold $\bar{y}_L$ is less than $1-\alpha$ (i.e., the probability that the load is below the threshold $\bar{y}_L$ is greater than α).

III. Solution of Stochastic Optimization Formulation

In this section we propose simulation-based and optimization-based (all-at-once) procedures to solve the stochastic optimization formulation.

A. Simulation-Based Search

The number of degrees of freedom u in the stochastic optimization problem is small (in our case these correspond to the controller parameters). Consequently, it is possible to perform an exhaustive search of the space $u \in \mathcal{U}$. This approach has the advantage that it allows us to explore the whole decision space and provides information on how power and maximum loads change with the controller parameters. Moreover, this approach is parallelizable and does not require derivative information. Consequently, with this approach we can handle non-smooth functions associated to the pitch and torque control laws and we can directly implement the IEC-61400 load extrapolation procedure. On the other hand, even when parallel simulations are used, a large number of simulations will be needed to span the entire decision space and the method will not scale. Scalability issues will become particularly evident when the wind turbine model is expensive to simulate or when more degrees of freedom need to be considered.

The simulation-based search procedure involves the following basic steps:

1) Given α, for each $u \in \mathcal{U}$, DO:
2) For each scenario wind scenario $V(t,\omega)$, simulate the dynamic model equations and compute expected power $\mathbb{E}\left[\frac{1}{T}\int_{\mathcal{T}} y_P(t,\omega)dt\right]$ and loads $y_L(t,\omega)$.
3) Use IEC-61400 load extrapolation procedure to match observed extreme load moments to moments of distribution.
4) Use moments to compute characteristic load $\hat{y}_L(\alpha)$.

After exploration of the entire control space $u \in \mathcal{U}$, determine the combination that maximizes expected power and satisfies the characteristic load constraint $\hat{y}_L(\alpha) \leq \bar{y}_L$.

B. Optimization-Based Search

In this, all-at-once approach, we discretize the wind turbine model to obtain a purely algebraic representation of the wind turbine model and with this we bypass the need to simulate the model repetitively. Another benefit of this approach is that we can obtain derivative information and handle a wider range of degrees of freedom and constraints (e.g., to consider different parameters in which an MPC controller overrides low-level controllers). The presence of non-smooth pitch and torque controller laws, however, requires of suitable smooth reformulations. Moreover, the load IEC-61400 extrapolation procedure requires an automated procedure to simultaneously extract multiple local maxima from load profiles to fit the long-term extreme value distribution while simultaneously maximizing power. This is inherently a *dual control problem* that seeks to maximize power while maximizing information extraction to perform long-term load inference. We now describe modifications to address these technical issues.

We reformulate the torque controller by using the non-smooth system of equations:

$$f_1(t) = \kappa w_g(t)^2 \tag{III.14a}$$

$$f_2(t) = \kappa w_{g_b}^2 + \frac{P_{rated}/w_{g_{25}} - \kappa w_{g_b}^2}{w_{g_{25}} - w_{g_b}}(w_g(t) - w_{g_b}) \tag{III.14b}$$

$$f_3(t) = P_{rated}/w_g(t) \tag{III.14c}$$

$$f_4(t) = \max\{f_1(t), f_2(t)\} \tag{III.14d}$$

$$T_{gen}(t) = \min\{f_4(t), f_3(t)\}. \tag{III.14e}$$

The $\min$ and $\max$ functions are approximated using this smooth functions:

$$f_4(t) = f_1(t) + \frac{1}{\epsilon}\log(1 + e^{-\epsilon(f_1(t)-f_2(t))}) \tag{III.15a}$$

$$T_{gen}(t) = f_3(t) - \frac{1}{\epsilon}\log(1 + e^{-\epsilon(f_4(t)-f_3(t))}) \tag{III.15b}$$

where $\epsilon > 0$ is the smoothing parameter. The $\max$ functions used in the pitch controller are approximated using the same approach.

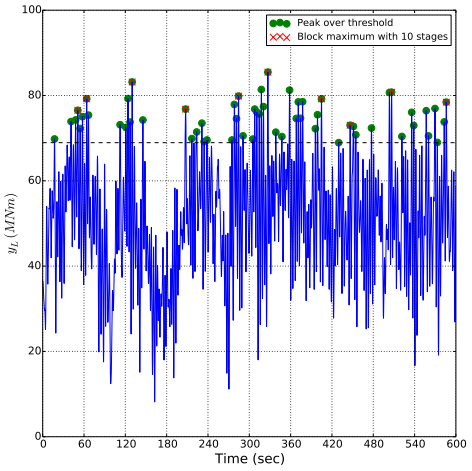

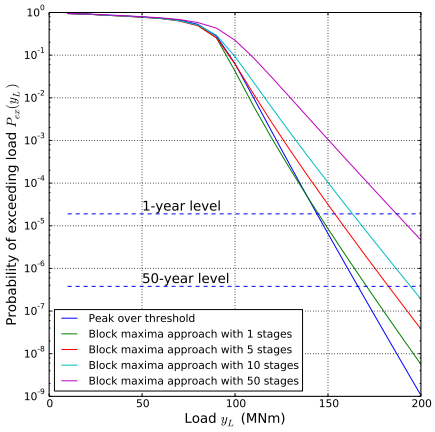

Fig. 2: **Extreme loads (top) and extreme value distributions (bottom) for peak over threshold and block maxima approaches.**

To implement the IEC-61400 procedure in an optimization setting, we use the so-called *block maximum* approach instead

of the *peak-over-threshold* approach described before. Here, we partition the horizon in $\mathcal{S} := \{1..S\}$ stages of length T/S and extract the maximum load in each stage. The sets $\mathcal{T}_s$ is the time domain of stage s and satisfy $\cup_{s\in\mathcal{S}}\mathcal{T}_s = \mathcal{T}$. We extract a total of S load maxima per wind realization and we denote the maximum load in stage $s \in \mathcal{S}$ and realization ω as $\eta_s(\omega)$. We recall that the maximum loads are categorized by wind speed level by splitting the realization set into subsets $\Omega_j,\ j \in \mathcal{B}$. Figure 2a illustrates how the *peak-over-threshold* and *block maximum* approaches select peak load values. Figure 2b compares the characteristic load obtained using these approaches for different number of stages. We can see that the characteristic load calculation using one stage in the block maximum method is close to that of the peak-over-threshold method.

The formulation (III.16) implements the proposed block-maximum load extrapolation procedure.

$$\min_{u\in\mathcal{U}} \sum_{s\in\mathcal{S}} \mathbb{E}\left[\eta_s(\omega)\right] \tag{III.16a}$$

$$\text{s.t. } (y_P(t,\omega), y_L(t,\omega)) = \phi(u, V(t,\omega)),\ t \in \mathcal{T},\ \omega \in \Omega \tag{III.16b}$$

$$y_L(t,\omega) \le \eta_s(\omega),\ \omega \in \Omega, t \in \mathcal{T}_s,\ s \in \mathcal{S} \tag{III.16c}$$

$$0 \le \eta_s(\omega),\ \omega \in \Omega,\ s \in \mathcal{S} \tag{III.16d}$$

$$\overline{L}_j = \frac{1}{|\mathcal{S}||\Omega_j|} \sum_{s\in\mathcal{S}} \sum_{\omega\in\Omega_j} \eta_s(\omega),\ j \in \mathcal{B} \tag{III.16e}$$

$$\sigma_j^2 = \frac{1}{|\mathcal{S}||\Omega_j|} \sum_{s\in\mathcal{S}} \sum_{\omega\in\Omega_j} (\eta_s(\omega) - \overline{L}_j)^2,\ j \in \mathcal{B} \tag{III.16f}$$

$$c_j = \frac{\sqrt{6}\,\sigma_j}{\pi},\ j \in \mathcal{B} \tag{III.16g}$$

$$L_j^0 = \overline{L}_j - c_j\gamma,\ j \in \mathcal{B} \tag{III.16h}$$

$$F_j = \exp - \left(\exp - \left(\frac{\hat{y}_L - L_j^0}{c_j}\right)\right),\ j \in \mathcal{B} \tag{III.16i}$$

$$P_{ex} = \sum_{j\in\mathcal{B}} p_j(1 - F_j^S) \tag{III.16j}$$

$$P_{ex} \le \alpha \tag{III.16k}$$

$$\hat{y}_L \le \bar{y}_L \tag{III.16l}$$

$$\mathbb{E}\left[\frac{1}{T}\int_{\mathcal{T}} y_P(t,\omega)dt\right] \ge \bar{P}. \tag{III.16m}$$

We treat this problem as a bi-objective problem that seeks to extract the maximum power while extracting maximum peak load information to perform long-term load extrapolation. We highlight that these objectives are conflicting because maximum power occurs at the maximum load. Because of this, the expected power is handled through the constraint (III.16m), where $\bar{P}$ is a minimum power level. The probability of exceedance $P_{ex}(y_L)$ is close to zero and this introduces numerical difficulties. To deal with this, we approximate $P_{ex}(y_L)$ using the form:

$$\begin{aligned} P_{ex}(y_L) &= \sum_{j\in\mathcal{B}} p_j(1 - F_j(y_L)^S) \\ &= \sum_{j\in\mathcal{B}} p_j(1 + F_j(y_L) + \ldots + F_j(y_L)^{S-1})(1 - F_j(y_L)) \\ &\approx \sum_{j\in\mathcal{B}} p_j(1 - F_j(y_L)), \end{aligned} \tag{III.17}$$

which is much easier to handle computationally.

C. Model Implementation in PLASMO

We use PLASMO to implement the stochastic optimization formulation. PLASMO (Platform for Scalable Modeling and Optimization) is a Julia-based modeling framework that facilitates the construction and analysis of structured optimization models. To do this, it leverages a hierarchical graph abstraction wherein nodes and edges can be associated with individual optimization models that are linked together [12]. Given a graph structure with models and connections, PLASMO can produce either a pure (flattened) optimization model to be solved using off-the-shelf optimization solvers such as IPOPT [13], or it can communicate graph structures to parallel solvers such as PIPS-NLP [14] and thus enable decomposition. PLASMO leverages the basic algebraic modeling syntax and automatic differentiation capabilities of JuMP [15]. By using a graph representation, automatic differentiation can be performed separately on each model associated to a given node. Moreover, by using a graph abstraction we can create sophisticated operations on individual nodes. For instance, we can warm-start a large-scale stochastic optimization problem by first finding solutions for individual scenario subproblems.

A two-stage stochastic nonlinear programming (NLP) problem induces a two-level hierarchical graph where in the parent node is a model that contains global variables and constraints (first-stage) while the children nodes are connected to the parent and contain their own model with local variables and constraints (second-stage or recourse). In this case, each children node corresponds to the model of each scenario or partition. In the case of the stochastic NLP with linking constraints (as those induced by the constraint (III.16j)), we can still pose the problem as a two-level graph by adding the coupling constraints and linking constraints to the parent node.

The code snippet shown in Figure 3 illustrates the implementation of problem (III.16) in PLASMO. As can be seen, the individual scenario models are created and appended to the parent node *on-the-fly* to create a two-level graph structure. The structure is directly communicated to PIPS-NLP, which uses a parallel Schur decomposition approach to solve the problem [14]. Note also that, under this modeling framework, the user does not need to have any knowledge on parallel computing. From the snippet we also note that PLASMO can also create a general (unstructured) NLP to be solved by off-the-shelf solvers like IPOPT [13]. This allows the user to compare computational performance and evaluate, for instance, if parallelization actually pays off.

```
#call libraries
using Plasmo
using JuMP

#initialize MPI
MPI.Init()

# create two-stage model
stom=graphModel()

# define first-stage variables in parent node
@variable(stom,P_rated)
@variable(stom,wg_ref)
@variable(stom,wg_2)
@variable(stom,wg_25)

# define auxiliary variables in parent node
@variable(stom,ȳ[Vbin])
@variable(stom,Var[Vbin])
@variable(stom,c[Vbin])
@variable(stom,L0[Vbin])
@variable(stom,F[Vbin])
@variable(stom,yL <=yȳ)
@constraint(stom,ccons[j in Vbin], c[j]==sqrt(6*Var[j])/pi)
@constraint(stom,Lcons[j in Vbin], L0[j]==ȳ[j] - c[j]*γ)
@constraint(stom,Fcons[j in Vbin], F[j]== exp(- exp(- (yL-L0[j])/c[j])))
@constraint(stom, sum{ p[j]*nb*(1-F[j]), j in Vbin} ≤ α )

# create array of scenario models
sm=Array(JuMP.Model,n)
for j in Vbin
    for k in Ω[j]
        # get scenario model and append to parent node
         sm[k] = get_scenario_model(k)
        @addNode(stom,sm[k])
        # add second-stage variables, constraints and objective to children scenario node
        @variable(sm[k],ȳ_local)
        @variable(sm[k],sq[1:nb])
        @constraint(sm[k],sqcons[b in 1:nb], sq[b]==(getvar(sm[k],:η[b])-ȳ_local)^2 )
        @objective(sm[k], sum{getvar(sm[k],:η[b]), b = 1:nb})
        # connect children and parent variables
        @constraint(stom, getvar(sm[k],:P_rated)==P_rated)
        @constraint(stom, getvar(sm[k],:wg_ref)==wg_ref)
        @constraint(stom, getvar(sm[k],:wg_2)==wg_2)
        @constraint(stom, getvar(sm[k],:wg_25)==wg_25)
        @constraint(stom, getvar(sm[k],:ȳ_local)==ȳ[k])
     end
end
 # add linking constraints to parent node
@constraint(stom,ȳcons[j in Vbin],ȳ[j]=sum{getvar(sm[k],:η)[b],k in Ω[j], b in 1:nb}/length(Ω[j])/nb)
@constraint(stom,Vcons[j in Vbin], Var[j]=sum{getvar(sm[k],:sq)[b],k in Ω[j], b in 1:nb}/length(Ω[j])/nb)
@constraint(stom,sum{p[j]*getvar(sm[k],:Power)[t]/length(Ω[j]),j in Vbin,k in
    Ω[j],t in Time}/length(Time) ≥ P̄ )

# solve structured with PIPS-NLP
ParPipsNlp_solve(stom)

# alternatively, solve structured problem as a general NLP with IPOPT
Ipopt_solve(stom)
```

Fig. 3: **Snippet of stochastic optimization implementation in** PLASMO

IV. Case Studies and Results

In this section we compare power and load profiles obtained with nominal and optimal controller parameters obtained with a simulation-based and an optimization-based search.

A. Simulation-Based Search

We first show the results of simulation-based search, which provides a rigorous (but computationally expensive) approach to search for optimal controller parameters. We discretize the control space $\mathcal{U}$ by using three points in each direction, which gives $3^4 = 81$ possible controller parameters. This number decreased to 30 by imposing constraints $w_{g_2} \leq w_{g_{25}} \leq w_{g_{ref}}$. For each controller setting, we perform 230 simulations to calculate the mean power output as well as the 50-year and 1-year characteristic loads using the peak-over-threshold approach reported in the IEC-61400 standard. The results obtained with the standard torque controller are shown in Table I. The simulations are parallelized by using 23 computing cores. Each point shown in the table corresponds to 230 simulations, and takes about 12 minutes of wall clock time using 23 computing cores. We use a multi-core computing server with Intel(R) Xeon(R) CPU E5-2698 v3 processors running at 2.30GHz. The entire set of results reported on the table take 5.8 hours of wall clock time. The sensitivity of the estimation of the mean power as well as of the 50-yr threshold on the number of scenarios are illustrated in Figures 4a and 4b. We can see that the confidence intervals stabilize at around 15-20 simulations per bin.

From Table I[1] we see that, given the load constraint $\hat{y}_L(\alpha_{50yr}) \leq \overline{y}_L = 200\,MNm$, the optimal controller parameters are $P_{rated} = 6\,MW, w_{g_{ref}} = 135.20\,rad/sec, w_{g_2} = 117.82\,rad/sec$, and $w_{g_{25}} = 133.85\,rad/sec$. The corresponding maximum expected power is $3.08\,MW$ and the characteristic load is $\hat{y}_L(\alpha_{50yr})$ =196 MNm. At an average electricity price of 30 USD/MWh, the total revenue collected by the turbine is 809,000 USD/yr (a total extracted power of 27 GWh/yr. In the first row of Table I) we present the performance of the turbine under base control parameters. Under these parameters, the expected power is $2.64MW$ and the load is 166 MNm. These base parameters yield an average annual revenue of 693,000 USD/yr (a total extracted power of 23 GWh/yr. The relative economic improvement is approximately 17.4% and we note that the base control parameters are conservative relative to the load threshold. These results highlight that the control parameters have a significant effect on the economic and structural performance of the turbine.

From Table I we can also observe that increasing P_{rated} and $w_{g_{ref}}$ increase both expected power and the characteristic load, while increasing $w_{g_{25}}$ decreases both expected power and the characteristic load. Increasing w_{g_2} decreases both expected power and characteristic load except when $P_{rated} = 5\,MW$ and $w_{g_{ref}} = 147.49\,rad/sec$, in which case the torque controller in region 2 becomes steeper than in region 2.5. This indicates non-monotonic behavior and highlights the need to develop advanced search procedures for control parameters.

B. Optimization-Based Search

The optimization-based approach can bypass the need to simulate the wind turbine model repetitively and can handle a wider range of degrees of freedom. For this approach, we discretize the model using a Radau collocation scheme [16]. To accurately capture extreme load values in the block maxima method, we have found that it is necessary to discretize the model using time steps of at least 0.5 seconds over 10 minutes, giving rise to 1,200 time steps. For an NLP with 230 scenarios, the total number of variables is 7.5 million. The models were implemented on `PLASMO` [12] and solved with `PIPS-NLP` [14]. The stochastic optimization problem is highly nonlinear and the minimum and maximum functions in the control laws introduce numerical difficulties. In particular, selecting an smoothing parameter ϵ is nontrivial (a large value of ϵ would cause solver difficulty while small value of ϵ results in low fidelity). In this work, we set $\epsilon = 1$. Despite of these complications, computational times reported in Table II show that the *optimization-based approach can reduce the computational time of the simulation-based search by a factor of two to four.* This clearly illustrates that bypassing the need to repetitively simulate the dynamic wind turbine model brings computational benefits.

The results of the optimization-based search are summarized in Table II and we also present a comparison with the results of the simulation-based search. The optimization formulation

[1]Due to restrictions in space, we only report a subset of the controller parameters.

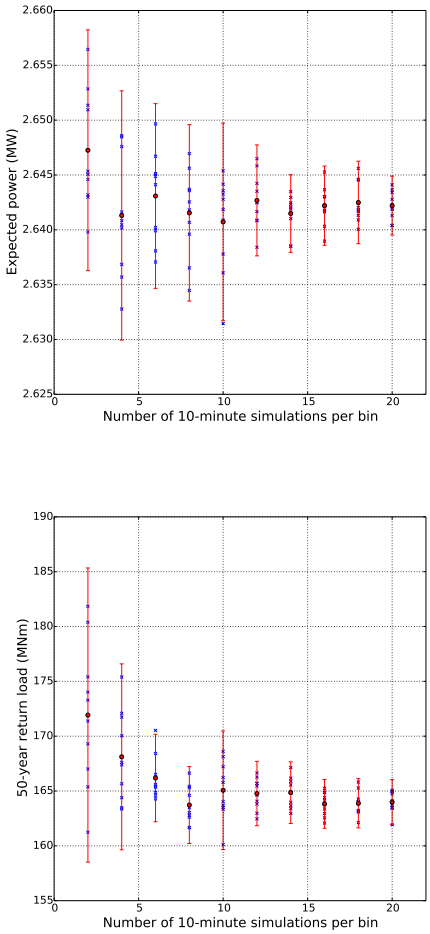

Fig. 4: **Expected power confidence levels (top) and 50-year characteristic load (bottom) confidence levels.**

uses a minimum power target $\bar{P}$ that is increased progressively. We validated the solution of the optimization-based search (which includes smoothed control laws and discretization) by fixing the controller parameters obtained and running simulations using 230 scenarios to compute expected power and characteristic load with standard peak-over-load threshold method. We observe that, while both the simulation-based search and optimization-based search push P_{rated} to its largest value of $P_{rated} = 6\,MW$ and push $w_{g_2} = 117.82\,rad/sec$ to the smallest value in the search region of w_{g_2}, the set-points for $w_{g_{ref}}$ and $w_{g_{25}}$ are quite different. The expected power obtained with optimization is 1% larger than that of the simulation-based search while the characteristic load of set-points from optimization is about 1% lower than that of the exhustive simulation based search. Figures 6 and 7 show the inputs and state profiles obtained with optimization, simulation with optimal set-points, and simulation with nominal set-points. Compared with the simulation approach with nominal set-points, the optimization approach clearly increases power output, the torque T_{gen}, and the load y_L while it decreases θ. We also observe that the profile obtained with optimization and the validation match fairly well, indicating that the approximations used in the optimization formulation are reasonable. The

TABLE I: **Expected power output and 1-yr and 50-yr characteristic loads for simulation-based search (using standard torque control law).**

P_{rated} (MW)	$w_{g_{ref}}$ (rad/sec)	w_{g2} (rad/sec)	w_{g25} (rad/sec)	y_P (MW)	$\hat{y}_L(\alpha_{50yr})$ (MNm)	$\hat{y}_L(\alpha_{1yr})$ (MNm)
5.0	122.91	117.82	121.68	2.64	166	144
5.0	135.20	117.82	121.68	2.83	208	176
		117.82	133.85	2.76	187	160
		129.60	133.85	2.73	182	157
5.0	147.49	117.82	121.68	2.85	225	189
		117.82	146.02	2.79	205	175
		129.60	146.02	2.80	208	177
		141.38	146.02	2.83	218	183
5.5	122.91	117.82	121.68	2.80	171	148
5.5	135.20	117.82	121.68	3.01	217	183
		117.82	133.85	2.93	191	165
		129.60	133.85	2.87	183	159
5.5	147.49	117.82	121.68	3.03	235	197
		117.82	146.02	2.96	211	180
		129.60	146.02	2.96	211	180
		141.38	146.02	2.97	212	181
6.0	122.91	117.82	121.68	2.94	175	152
6.0	135.20	117.82	121.68	3.18	226	190
		117.82	133.85	3.08	196	170
		129.60	133.85	3.02	187	163
6.0	147.49	117.82	121.68	3.20	246	206
		117.82	146.02	3.13	216	185
		129.60	146.02	3.12	214	183
		141.38	146.02	3.10	210	181

mismatch between the profiles is due to the time discretization of states and the smoothing of the control laws.

Based on the optimal parameters obtained with optimization, we have derived a heuristic control law. This consists of keeping both w_{g_2} and $w_{g_{25}}$ at the nominal value, and increase P_{rated} and $w_{g_{ref}}$. This heuristic is rarely mentioned in the literature. With only two degrees of freedom, we can discretize the space $\mathcal{U}$ using a finer mesh, as shown in Table III. Both $w_{g_{ref}}$ and P_{rated} are discretized with 6 points, resulting in $6^2 = 36$ combinations[2]. From Table III, we can conclude that the optimal setting P_{rated} is $6\,MW$ and the optimal setting $w_{g_{ref}}$ is 127.83 rad/sec. Compared with the nominal set-points, the optimal set-points increase the power output from $2.64\,MW$ to $3.12\,MW$ (improvement of 18%) and $\hat{y}_L(\alpha_{50yr})$ from 166 MNm to 196 MNm (increase of 18%). The approach illustrates how an optimization-based approach can be used to identify more effective heuristic search strategies. From these results we also observe that the characteristic load is more sensitive to the changes in $w_{g_{ref}}$ than the changes in P_{rated}. For example, increasing P_{rated} from $5\,MW$ to $6\,MW$ increases the expected power from 2.64 MW to 2.94 MW at the cost of increasing $\hat{y}_L(\alpha_{50yr})$ from $166MNm$ to $175MNm$. However, increasing $w_{g_{ref}}$ from $122.91\,rad/sec$ to $147.49\,rad/sec$ only increases the expected power 2.64 MW to 2.85 MW while increases $\hat{y}_L(\alpha_{50yr})$ from $166\,MNm$ to $225\,MNm$. The 1-year characteristic load $\hat{y}_L(\alpha_{1yr})$ is notably smaller than $\hat{y}_L(\alpha_{50yr})$. If we relax the load constraint to $\hat{y}_L(\alpha_{1yr}) \leq \overline{y}_L$, then the optimal $w_{g_{ref}}$ increases to $137.66\,rad/sec$ and the optimal power increases from $3.12\,MW$ to $3.19\,MW$ (an improvement of 2%).

[2]Due to restrictions in space, we only report a subset of these cases.

C. Effect of Pitch and Torque Control Laws

We have also used the proposed formulation to explore how the control law affects performance. Table IV shows the results using the modified torque controller in which we use the proposed heuristic to identify optimal parameters. An interesting observation is that, for almost all combinations of P_{rated} and $w_{g_{ref}}$, the change of control law has limited effect on the characteristic load but can increase the mean power output. With the load constraint $\hat{y}_L(\alpha_{50yr}) \leq \overline{y}_L = 200MNm$, the optimal P_{rated} is $6\,MW$ and the optimal $w_{g_{ref}}$ is 127.83 rad/sec, which are the same as those obtained with optimal set-points with the standard torque controller. However, by changing the control law of the generator torque in region 3 while using the same parameters, the corresponding expected power increases from $3.12\,MW$ to $3.24\,MW$ (an improvement of 3.8 %) while $\hat{y}_L(\alpha_{50yr})$ decreases from 196 to 193 MNm (a 1.5% change). By relaxing the load constraint to $\hat{y}_L(\alpha_{1yr}) \leq \overline{y}_L$, the expected power increases from $3.24\,MW$ to $3.51\,MW$.

Table V summarizes the results obtained with the optimization-based search using the modified torque controller. We see that the solution is fairly close to the that obtained with the rigorous simulation-based search. Here, we also show the results obtained with optimization using $S = 1$ and $S = 10$ stages in the block maxima method. Although the optimization using $S = 1$ and $S = 10$ stages result in the same solution, we also observe that the solution time obtained with $S = 10$ stages is significantly longer.

The difference between the results obtained using the standard and modified torque controller highlight that the *control law has a significant effect in performance*. To understand how strong this effect can actually be, we solved an optimization instance *without control laws*. That is, the time profile of the angle $\theta(t)$ and torque $T_{gen}(t)$ are used directly as decision

TABLE II: **Results for simulation-based and optimization-based search of controller parameters using standard torque control.**

Approach	$\bar{P}$ (MW)	P_{rated} (MW)	$w_{g_{ref}}$ (rad/sec)	w_{g_2} (rad/sec)	$w_{g_{25}}$ (rad/sec)	y_P (MW)	$\hat{y}_L(\alpha_{50yr})$ (MNm)	Solution Time (hr)
Simulation		6	135.20	117.82	133.85	3.08	196	5.8
Optimization	2.9	6	124.26	117.82	122.34	3.00	178	1.3
	3.0	6	125.79	117.82	121.68	3.07	187	2.8
	3.05	6	127.26	117.82	121.68	3.11	194	1.5

TABLE III: **Expected power output and characteristic loads using standard torque controller.**

$P_{rated}(MW)$	$w_{g_{ref}}(rad/sec)$	y_P (MW)	$\hat{y}_L(\alpha_{50yr})$ (MNm)	$\hat{y}_L(\alpha_{1yr})$ (MNm)
5.0	122.91	2.64	166	144
	132.74	2.83	203	172
	142.58	2.85	220	185
	147.49	2.85	225	189
5.4	122.91	2.77	170	148
	132.74	2.97	210	178
	142.58	2.99	228	191
	147.49	3.00	233	196
6.0	122.91	2.94	175	152
	127.83	3.12	196	169
	132.74	3.17	220	185
	142.58	3.19	240	201
	147.49	3.20	246	206

TABLE IV: **Expected power output and characteristic loads using modified torque controller.**

$P_{rated}(MW)$	$w_{g_{ref}}(rad/sec)$	y_P (MW)	$\hat{y}_L(\alpha_{50yr})$ (MNm)	$\hat{y}_L(\alpha_{1yr})$ (MNm)
5.0	122.91	2.70	166	145
	132.74	3.00	197	169
	142.58	3.15	217	185
	147.49	3.22	225	191
5.4	122.91	2.82	170	148
	132.74	3.15	203	174
	142.58	3.30	224	191
	147.49	3.37	233	198
6.0	122.91	3.00	174	152
	127.83	3.24	193	167
	132.74	3.35	211	181
	142.58	3.51	235	200
	147.49	3.58	244	207

variables. This can be interpreted as an *MPC control strategy*. We note that this induces a very large number of degrees of freedom (in this case 2,400). Consequently, a simulation-based search is no longer applicable. Table VI shows that the expected power obtained with MPC is 3.9 MW, *which represents an improvement of 25.9% relative to the optimal settings found with the use of control laws* (3.07 MW). The MPC strategy improves the annual power by 7 GWh/yr (at an electricity price of 30 USD/MWh this represents and improvement of 218,000 USD/yr. We also note that the solution times of the MPC strategy are reduced to 40 minutes, which highlight the complexity introduced by the non-smooth control laws. Although the deployment of the MPC strategy is more challenging, these results provide an idea of the potential performance. Moreover, the computational times indicate that it seems plausible that additional simplifications can be used to enable real-time MPC implementations. These results also highlight that the proposed optimization-based approach can be used as a research tool to investigate the benefits of using more advanced control architectures.

V. Conclusions and Future Work

We have proposed a general stochastic optimization formulation to identify optimal parameters for pitch and torque controllers that maximize power and mitigate long-term extreme loads in wind turbines. The proposed formulation incorporates a wind turbine dynamic model, control law representations for pitch and torque controllers, and a rigorous procedure to estimate the probability of long-term extreme load exceedance (as described by the IEC-61400 standard). We provide evidence that the approach can significantly improve performance of nominal controller parameters. We also demonstrate that the formulation can be solved efficiently by using parallel nonlinear interior-point solvers. As a part of future work, we are interested in exploring the effect of turbulence conditions in the estimation of long-term extreme loads and to incorporate higher fidelity wind turbine models.

Appendix A
Model Nomenclature

Differential states:

$w_r(t)$	: Rotor speed [rad/sec]
$x(t)$	: Tower top displacement fore-aft [m]
$v_x(t)$	: Velocity of x [m/sec]

Algebraic states:

$\lambda(t)$	: Effective tip speed ratio [-]
$C_t(t)$	: Thrust coefficient [-]
$C_m(t)$	: Power coefficient [-]
$F_z(t)$	: Aerodynamic thrust force [N]

TABLE V: **Results of simulation-based and optimization-based search with modified torque controller.**

Approach	$\bar{P}$ (MW)	P_{rated} (MW)	$w_{g_{ref}}$ (rad/sec)	y_P (MW)	$\hat{y}_L(\alpha_{50yr})$ (MNm)	Solution Time (hr)
Simulation		6	127.83	3.24	189	4.9
Optimization (1 stage)	3.0	6	124.39	3.09	180	1.8
	3.1	6	126.14	3.18	187	2.3
	3.2	6	128.49	3.26	196	3.3
Optimization (10 stages)	3.0	6	124.39	3.09	180	10.0
	3.1	6	126.14	3.18	187	7.8
	3.2	6	128.49	3.26	196	11.6

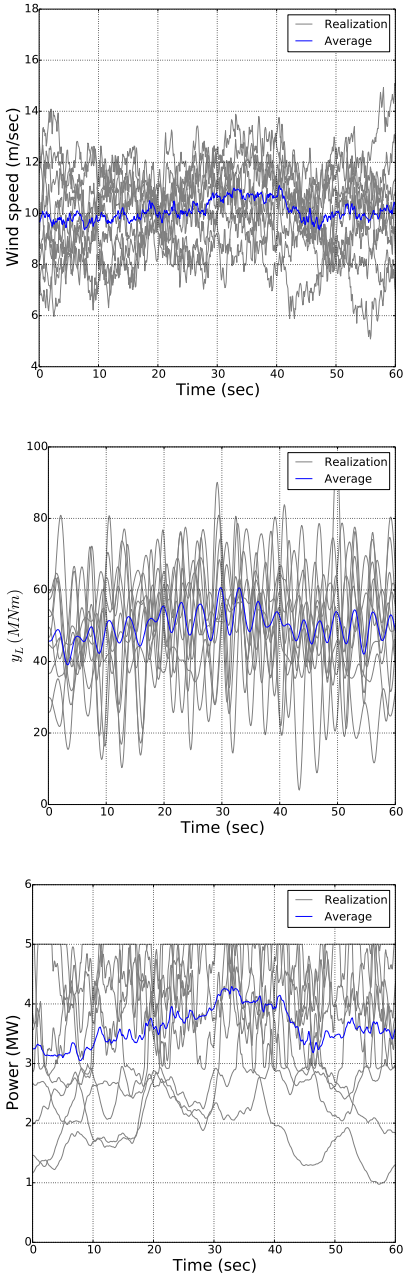

Fig. 5: **Wind, load, and power profiles for mean wind speed of** 10 **m/s.**

$M_z(t)$: Aerodynamic torque $[Nm]$

Disturbances and controls:
$V(t)$: Wind speed $[m/sec]$
$\theta(t)$: Collective pitch angle $[^\circ]$

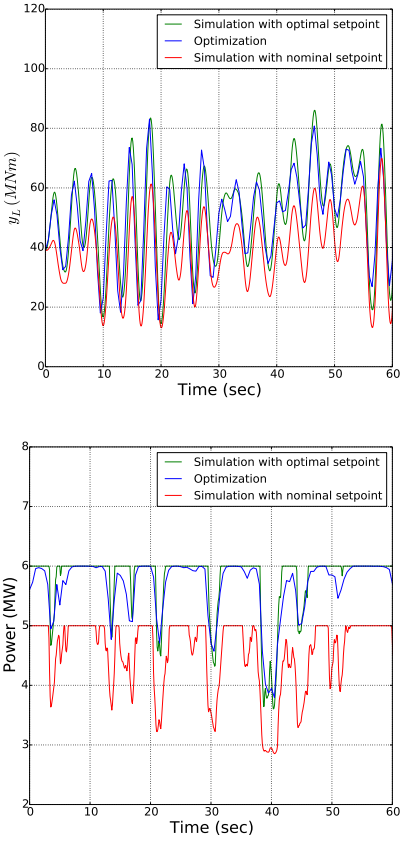

Fig. 6: **Power and load profiles at 15** m/sec**.**

TABLE VI: **Results of optimization without control laws.**

$\bar{P}$ (MW)	y_P (MW)	$\hat{y}_L(\alpha_{50yr})$ (MNm)	Solution Time (hr)
3.7	3.71	209	0.3
3.9	3.91	186	0.7

$T_{gen}(t)$: Generator torque (at high speed shaft) $[Nm]$

System outputs:
$y_P(t)$: Electrical power $[W]$
$y_L(t)$: Tower base bending moment (load) $[Nm]$

Parameters:
N_g = 97 : Gear ratio generator shaft [-]
R_r = 63 : Rotor radius $[m]$
$A = \pi R_r R_r$: Disk area $[m^2]$
J =11776047 : Total moment of inertia of the drive-train $[kgm^2]$
P_1 = 0.056 : P loss coefficient (linear) [-]
ρ = 1.225 : Air density $[kg/m^3]$
H = 90 : Tower height $[m]$
m_{Te} = 436750 : Tower equivalent modal mass $[kg]$
$\overline{y}_L$ = 200 : Maximum load threshold $[MNm]$

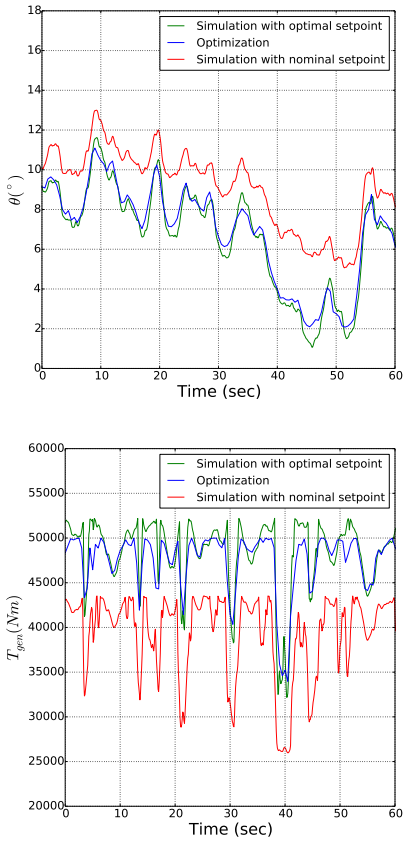

Fig. 7: **Pitch angle and torque 15** m/sec**.**

c_{Te} = 17782 : Tower structural damping $[kg/s]$
k_{Te} = 1810000 : Bending stiffness $[kg/s^2]$
P_{rated0} = 5 : Nominal rated power $[MW]$
$w_{r_{rated0}}$ = 1.267 : Nominal rated rotor speed $[rad/sec]$
$w_{g_{rated0}}$ = 122.91 : Nominal rated generator speed $[rad/sec]$
$w_{g_{ref0}}$ = 122.91 : Nominal reference generator speed $[rad/sec]$
w_{g20} = 117.82 : Nominal boundary speed $[rad/sec]$
w_{g250} = 121.68 : Nominal boundary speed $[rad/sec]$
V_{rated} = 11.2 : Rated wind speed $[m/sec]$
λ_{opt} = 8.22 : Optimal tip speed ratio [-]
cp_{max} = 0.51 : Peak power coefficient [-]
θ_{min} = 0 : Minimum blade pitch angle $[^\circ]$
θ_{max} = 30 : Maximum blade pitch angle $[^\circ]$

REFERENCES

[1] P. J. Moriarty, W. Holley, and C. P. Butterfield, *Extrapolation of extreme and fatigue loads using probabilistic methods*. National Renewable Energy Laboratory, 2004.

[2] P. Ragan and L. Manuel, "Statistical extrapolation methods for estimating wind turbine extreme loads," *Journal of Solar Energy Engineering*, vol. 130, no. 3, p. 031011, 2008.

[3] H. S. Toft, J. D. Sørensen, and D. Veldkamp, "Assessment of load extrapolation methods for wind turbines," *Journal of Solar Energy Engineering*, vol. 133, no. 2, p. 021001, 2011.

[4] E. Bossanyi, "Wind turbine control for load reduction," *Wind energy*, vol. 6, no. 3, pp. 229–244, 2003.

[5] J. H. Laks, L. Y. Pao, and A. D. Wright, "Control of wind turbines: Past, present, and future," in *American Control Conference, 2009.* IEEE, 2009, pp. 2096–2103.

[6] U. Jassmann, J. Zierath, S. Dickler, and D. Abel, "Model predictive wind turbine control for load alleviation and power leveling in extreme operation conditions," in *Control Applications (CCA), 2016 IEEE Conference on*. IEEE, 2016, pp. 1368–1373.

[7] D. Schlipf, D. J. Schlipf, and M. Kühn, "Nonlinear model predictive control of wind turbines using lidar," *Wind Energy*, vol. 16, no. 7, pp. 1107–1129, 2013.

[8] P. F. Odgaaard and T. G. Hovgaard, "On practical tuning of model uncertainty in wind turbine model predictive control," *IFAC-PapersOnLine*, vol. 48, no. 30, pp. 327–332, 2015.

[9] M. Soltani, R. Wisniewski, P. Brath, and S. Boyd, "Load reduction of wind turbines using receding horizon control," in *Control Applications (CCA), 2011 IEEE International Conference on*. IEEE, 2011, pp. 852–857.

[10] E. Tofighi, D. Schlipf, and C. M. Kellett, "Nonlinear model predictive controller design for extreme load mitigation in transition operation region in wind turbines," in *2015 IEEE Conference on Control Applications (CCA)*. IEEE, 2015, pp. 1167–1172.

[11] J. Jonkman, S. Butterfield, W. Musial, and G. Scott, "Definition of a 5-mw reference wind turbine for offshore system development," *National Renewable Energy Laboratory, Golden, CO, Technical Report No. NREL/TP-500-38060*, 2009.

[12] J. Jalving, S. Abhyankar, K. Kim, M. Hereld, and V. M. Zavala, "A graph-based computational framework for simulation and optimization of coupled infrastructure networks," *Undr Review*, 2016.

[13] A. Wächter and L. T. Biegler, "On the implementation of a primal-dual interior point filter line search algorithm for large-scale nonlinear programming," *Mathematical Programming*, vol. 106, pp. 25–57, 2006.

[14] N.-Y. Chiang and V. M. Zavala, "An inertia-free filter line-search algorithm for large-scale nonlinear programming," *Computational Optimization and Applications*, vol. 64, no. 2, pp. 327–354, 2016.

[15] M. Lubin and I. Dunning, "Computing in operations research using julia," *INFORMS Journal on Computing*, vol. 27, no. 2, pp. 238–248, 2015.

[16] V. M. Zavala, *Computational strategies for the optimal operation of large-scale chemical processes*. ProQuest, 2008.